Article

Geological Conditions Evaluation of Coalbed Methane of Dacun Block in the Guxu Mining Area, Southern Sichuan Coalfield

Xushuang Zhu [1], Zheng Zhang [2,*], Yonggui Wu [1], Zhengjiang Long [1] and Xiaodong Lai [1]

1 The 6th Geological Brigade of Sichuan, Luzhou 646000, China; zhuxushuang@126.com (X.Z.);
wuyongguiscd6@163.com (Y.W.); 18090603869@163.com (Z.L.); 18715847573@163.com (X.L.)
2 Key Laboratory of Coalbed Methane Resources and Reservoir Formation Process, Ministry of Education,
China University of Mining and Technology, Xuzhou 221116, China
* Correspondence: zzcumt@cumt.edu.cn

Abstract: The geological conditions evaluation of coalbed methane (CBM) is of great significance to CBM exploration and development. The CBM resources in the Southern Sichuan Coalfield (SSC) of China are very abundant; however, the CBM investigation works in this area are only just beginning, and the basic geological research of CBM is seriously inadequate, restricting CBM exploration and development. Therefore, in this study, a representative CBM block (Dacun) in the SSC was selected, and the CBM geological conditions were evaluated based on field injection/fall-off well testing, gas content and composition measurements, and a series of laboratory experiments. The results show that the CH_4 concentrations of coal seams in the Dacun Block, overall, take on an increasing trend as the depth increases, and the CH_4 weathering zone depth is 310 m. Due to the coupled control of temperature and formation pressure, the gas content shows a "increase→decrease" trend as the depth increases, and the critical depth is around 700 m. The CBM is enriched in the hinge zone of the Dacun syncline. The moisture content shows a negative correlation with CBM gas content. The porosities of coal seams vary from 4.20% to 5.41% and increase with the $R_{o,max}$. The permeabilities of coal seams show a strong heterogeneity with values ranging from 0.001mD to 2.85 mD and present a decreasing trend with the increase in depth. Moreover, a negative relationship exists between coal permeability and minimum horizontal stress magnitude. The reservoir pressure coefficients are between 0.51 and 1.26 and show a fluctuation change trend (increase→decrease→increase) as the depth increases, reflecting that three sets of independent superposed gas-bearing systems possibly exist vertically in the Longtan Formation of the study area. The Langmuir volumes (V_L) of coals range from 22.67 to 36.84 m^3/t, indicating the coals have strong adsorptivity. The V_L presents a parabolic change of first increasing and then decreasing with the increase in depth, and the turning depth is around 700 m, consistent with the critical depth of gas content. The gas saturations of coal seams are, overall, low, with values varying from 29.10% to 116.48% (avg. 68.45%). Both gas content and reservoir pressure show a positive correlation with gas saturation. The CBM development in the Dacun Block needs a large depressurization of reservoir pressure due to the low ratio (avg. 0.37) of critical desorption pressure to reservoir pressure.

Keywords: coalbed methane; geological condition; Dacun Block; Southern Sichuan Coalfield

1. Introduction

Influenced by remarkable changes in the global energy pattern, the accelerated adjustment of the global energy structure, and the domestic goal of carbon peaking and carbon neutrality, the development of clean energy has ushered in a period of important strategic opportunities in China [1,2]. Accelerating the development of unconventional natural gasses such as coalbed methane (CBM) and shale gas is of great significance to strengthening the security guarantee of China's energy strategy and consolidating the foundation of resource supply guarantees [3]. Many nations that produce coal, like the

Australia, Canada, USA, China, and so on, have favored CBM [4–6] as a type of clean and highly efficient energy [7] as well as an important chemical material [8].

After more than 20 years of exploration, the CBM industry in China has begun to take shape, and two major CBM industrial bases, Southern Qinshui Basin (SQB) and Eastern Ordos Basin (EOB), have been built [9,10]. Moreover, the CBM exploration and development in the Southern Junggar Basin [11], Western Guizhou [12], Eastern Yunan [13], and Erlian basin [14] of China is also being carried out and thriving. The total number of surface CBM wells in China has exceeded 20,000 at present, and the total CBM production has achieved 117.7×10^8 m^3 in 2023, which mainly comes from SQB and EOB.
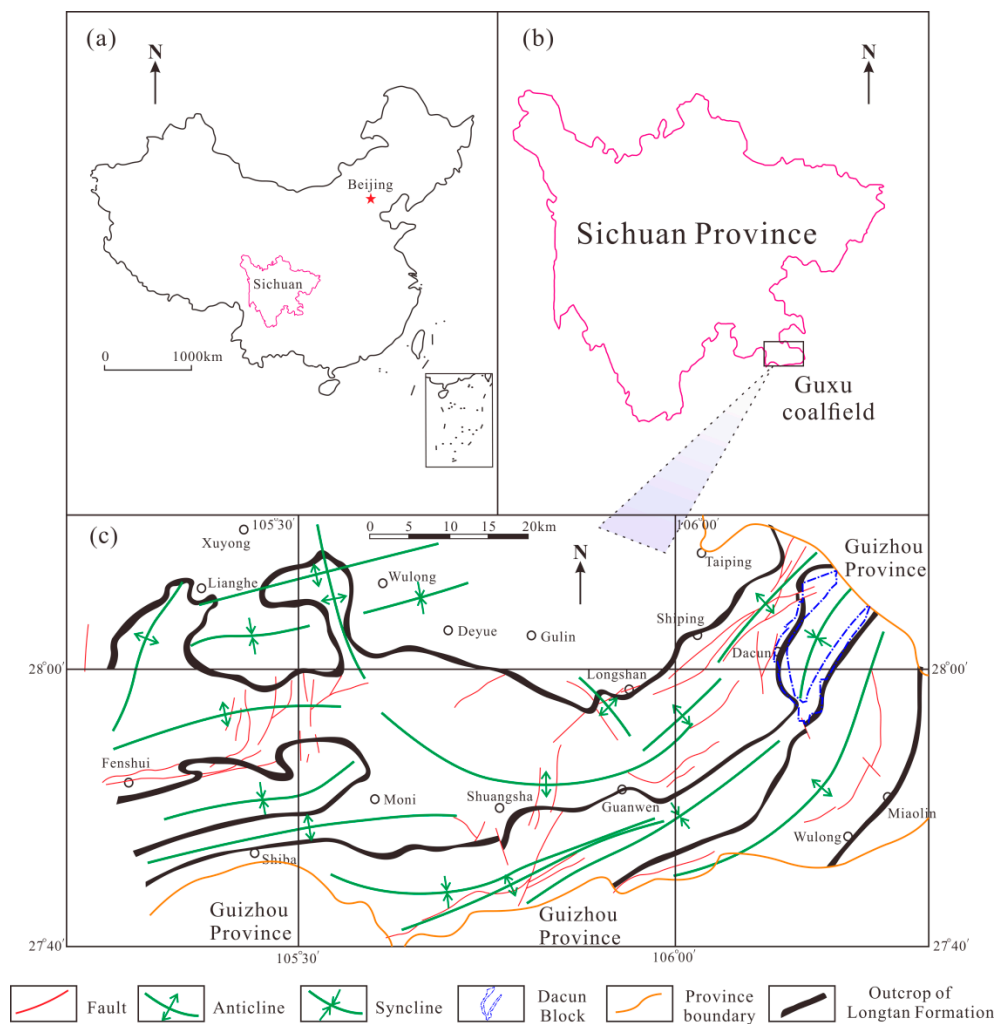
Unlike conventional natural gas, CBM is primarily stored in coal reservoirs through adsorption [15]. As a special organic rock mass, coal reservoirs are featured with developed pore and cleat system [16,17], low mechanical strength [18,19], strong heterogeneity [20,21], etc. Meanwhile, coal reservoirs are very sensitive to pressure, temperature, and stress, leading to evident planar and vertical variations in CBM accumulation and development conditions [22–24]. The CBM accumulation in coal reservoirs is attributed to the synergistic effect of many geological factors, such as burial depth, coal rank, coal thickness, coal quality, coal adsorptivity, sealing condition, hydrogeology, structural condition, etc. [22,24–28]. The CBM development is also influenced by many geological factors, such as gas content, gas saturation, coal permeability, porosity, critical desorption pressure, etc. [29–31]. Thus, the geological conditions evaluation of CBM is of great significance to CBM exploration and development.

It is estimated that the total CBM resources, less than 2000 m in depth in the Sichuan Province of China, are 6715×10^8 m^3, among which approximately 67% are in the Southern Sichuan Coalfield (SSC) [32]. However, the CBM exploration, development, and utilization works in the SSC started late and progressed slowly, and the basic geological research on CBM is seriously inadequate. The Guxu mining area is one of the few areas that have conducted CBM geological evaluation works in the SSC. Analyzing and evaluating the geological conditions of CBM can not only guide CBM exploration and development in the Guxu mining area; it can also play a positive demonstrative role for other CBM target areas of SSC.

In this study, the Dacun Block of the Guxu mining area was selected as the objective area, and the CBM geological conditions, including gas content, gas saturation, porosity, permeability, reservoir pressure, adsorption capacity, and critical desorption pressure, were analyzed and discussed. The works in this study could provide a guide for the target area selection of CBM enrichment and high production in the Dacun Block and then promote the exploration and development of CBM in the Guxu mining area.
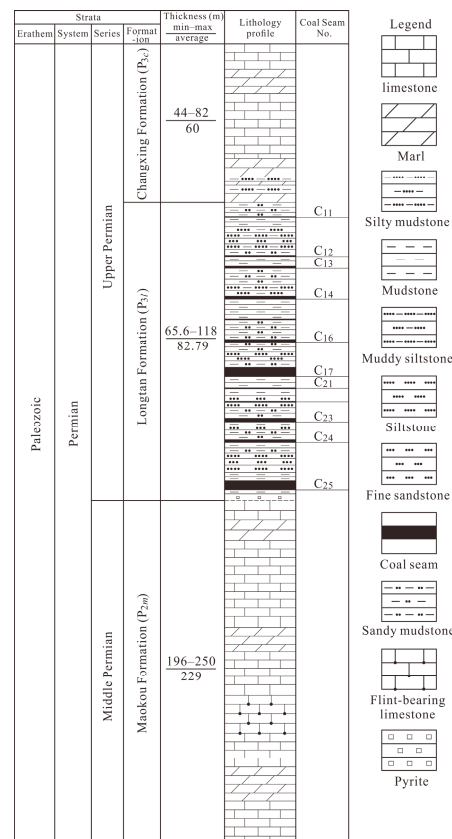
2. Geological Settings

The Guxu mining area of SSC is administratively subordinate to the Gulin County and Xuyong County of Luzhou City, Sichuan Province (Figure 1a,b), and it is divided into eleven blocks, such as Lianghe, Gulin, Dacun and Heba. The Guxu mining area is tectonically located in the Xuyong–Junlian superimposed fold belt on the southern margin of the Sichuan foreland basin, and it is mainly composed of Gulin anticlinorium and several secondary folds (Figure 1c). The faults with a main NE strike are well developed in the hinge zone and two limbs of Gulin anticlinorium, and most of the faults are reverse faults. The study area, Dacun Block, is, on the whole, a synclinal structure (Dacun syncline). The axis of the Dacun syncline is nearly SN at the southern section, and NE–SW at the middle and north sections. The dip angle of the formation in the Dacun Block is generally 30–50° and can maximally reach 85° in the local areas. The secondary folds are not developed in the Dacun block; the faults are mainly developed in the northwest and south parts of the block (Figure 1c); it is proved through investigations that most faults in the Dacun Block do not cut coal seams.

Figure 1. (**a**) Location of Sichuan Province in China. (**b**) Location of Guxu coalfield in Sichuan Province. (**c**) The major structures in the Guxu coalfield and the location of the Dacun Block in the Guxu coalfield.

The strata outcropped in the Dacun Block include Silurian, Permian, Jurassic, and Quaternary from the bottom to the top. The coal-bearing stratum is the Upper Permian Longtan Formation (P_{3l}), which is deposited in an interactive marine and terrestrial environment. The lower part of P_{3l} is deposited in a lagoon-tidal flat environment, and the middle and upper parts are deposited in a delta-tidal flat environment [33]. The thickness of P_{3l} ranges from 65.60m to 118m, with an average of 82.79m (Figure 2). The P_{3l} is mainly composed of mudstone, sandy mudstone, muddy siltstone, siltstone, fine sandstone and coal, and carbonaceous mudstone.

The P_{3l} in the Dacun Block has a good coal-bearing property with a large number of coal layers and a stable thickness of main coal seams. The coal seams usually have a simple structure with 0–3 layers of gangues. More than 20 coal seams occur in the P_{3l} of study area, and among them, 9 coal seams can be compared regionally and are numbered C_{11}, C_{13}, C_{14}, C_{16}, C_{17}, C_{21}, C_{23}, C_{24}, and C_{25} from top to bottom. Among them, C_{13}, C_{14}, C_{16}, C_{17}, C_{23}, C_{24}, and C_{25} are commercial coal seams. The total thickness (excluding gangue) of coal seams in the P_{3l} varies from 4.35m to 19.76m (avg. 10.99 m), accounting for 6.35–21.47% (avg. 13.42%) of the total thickness of P_{3l}.

Figure 2. Comprehensive stratigraphic column of Permian coal measures in the Dacun Block.

The macrolithotypes of coals in the Dacun block are dominated by semi-dull coals (including C_{13}, C_{14}, C_{16}, C_{17}, and C_{23}), followed by semi-bright coals (including C_{21}, C_{24}, and C_{25}). The true and apparent densities of coals range from 1.20 to 1.98 g/cm^3 (avg. 1.60 g/cm^3) and 1.35 to 1.83 g/cm^3 (avg. 1.54 g/cm^3), respectively. The organic macerals of coals are dominated by vitrinite (vol. 59.12–88.74%; avg. 73.35%), followed by inertinite (vol. 11.26–40.88%; avg. 26.65%), and exinite is generally rare. The minerals in coals account for 10.80–44.60% (avg. 25.48%) of the total volume and are mainly composed of clay minerals, followed by calcite and sulfide. Proximate analysis shows that the moisture contents (M_{ad}) of coals vary from 0.25 to 5.27% (avg. 1.30%); ash yields (A_d) at 8.87–39.55% (avg. 23.92%), volatile yields (V_d) at 4.96–30.32% (avg. 7.80%); and fixed carbon content (FC_d) at 12.95–83.24% (avg. 68.29%). The calorific values of coals are between 16.03 and 32.19 MJ/kg, averaging 26.30 MJ/kg. The maximum reflectance of vitrinite ($R_{o,max}$) of coals ranges from 2.59% to 3.10% (avg. 2.82%), indicating that the coals in the study area are semi-anthracite to anthracite in coal rank.

3. Materials and Methods

3.1. Core Data

The measured gas content, porosity, coal proximate and petrographic analyses, and Langmuir Isotherm adsorption data were collected from the CBM wells in the Dacun Block. The porosity was measured using the helium expansion method according to Chinese Standard SY/T5336-1996 [34]. The coal proximate, including moisture, ash yield, volatile matter, and fixed carbon, were conducted using a 5E-MAC III infrared fast core analyzer and performed following ASTM Standards D3173–11 [35] and D3174–11 [36]. The $R_{o,max}$ was performed using a Leitz MPV-3 photometer microscope based on the Standard of ISO7404.5-1994 [37].

The Langmuir Isotherm adsorption experiments were conducted based on Chinese standard GB/T 19560-2004 [38]. All coal samples were crushed and sieved to a size range of

60–80 mesh, and then 100–125 g samples were subjected to moisture equilibrium treatment. The moisture equilibrium treatment was processed for at least four days for each sample. After these pretreatments, the coals were put into the sample cell of the IS-100 for the adsorption isotherm experiment. The experimental temperature and equilibrium pressure were 30 °C and up to 10 MPa.

In this work, the total gas content (Q_t) data of coal samples were determined based on the direct method of United States Bureau of Mines (USBM) [39], and they consisted of three parts: (1) the measured desorbed gas (Q_1) in desorption canisters; (2) the measured residual gas (Q_2) released during the crushing of coal sample; and (3) the lost gas (Q_3) estimated based on Q_1; that is, $Q_t = Q_1 + Q_2 + Q_3$. The Qt in this work is reported on a d.a.f. basis.

The gas saturation was calculated through the following equation:

$$S = \frac{V_a(p + p_L)}{V_L p},$$ (1)

where S is gas saturation, in %; V_a is the measured gas content of coal seam, in m^3/t; p is the measured reservoir pressure, in MPa; p_L is the Langmuir pressure, in MPa; and V_L is the Langmuir volume, in m^3/t.

3.2. Gas Composition Data

In this work, a total of 58 gas composition samples were collected in the Dacun Block. The gas composition samples were obtained from the inverted cylinders and generally taken at early and mid-stages of desorption. The gas composition samples were analyzed on a GC-2014 Gas Chromatograph Manufactured by Shimadzu. In this study, the average values of gas compositions of samples at early and mid-stages of desorption were taken as the gas composition results.

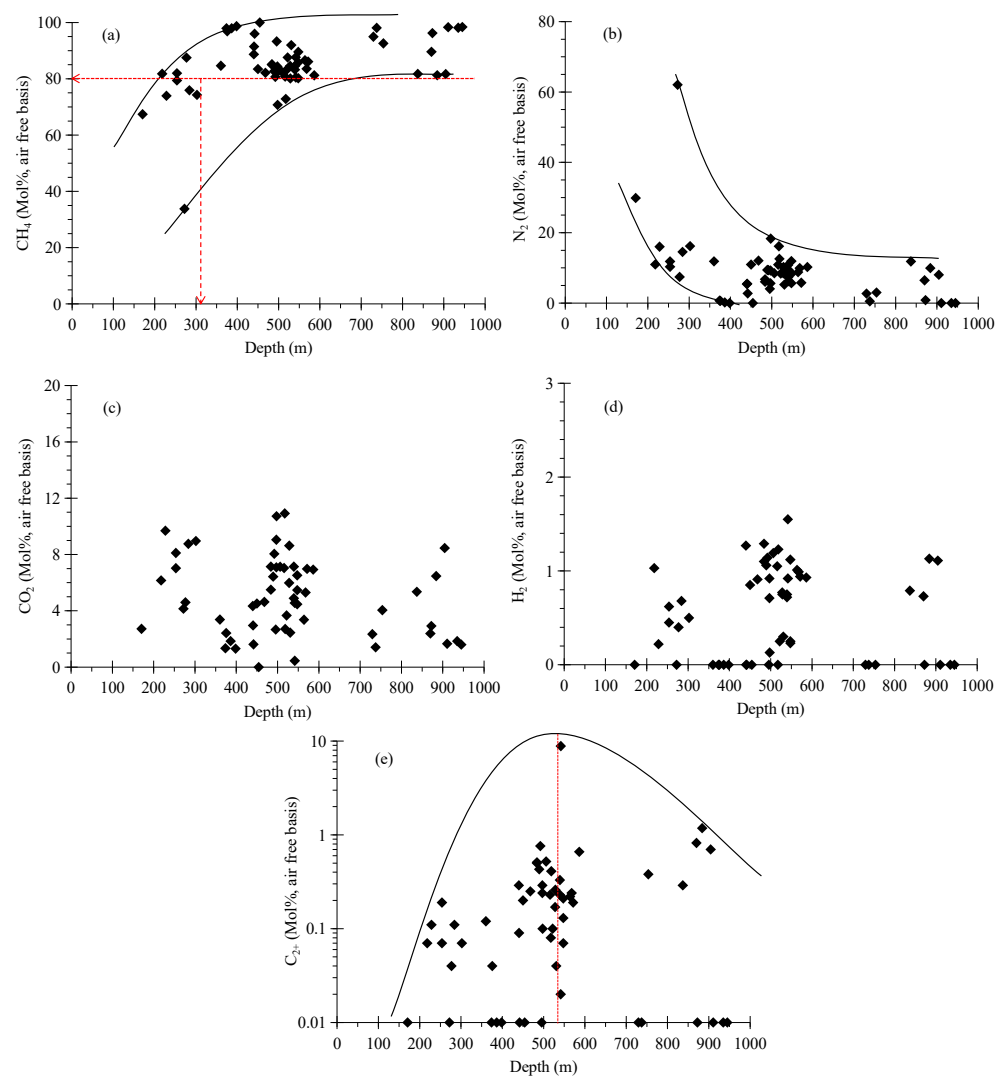### 3.3. Insitu Reservoir Pressure, Stress, and Permeability Data

The insitu reservoir pressure, stress, and permeability data of CBM wells in the Dacun Block were collected, and these data were obtained through injection/fall-off well testing conducted via a coal geological engineering survey and design institute in Sichuan. The injection/fall-off well testing is a single-well pressure transient test, in which a certain amount of water is injected into the reservoir at a constant rate for a period of time and then the well is shut in for pressure recovery. The bottom hole pressure data during injection and shut-in are recorded, respectively, and the reservoir parameters, such as insitu reservoir pressure, stress, and permeability data, are calculated through this test.

4. Results and Discussions

4.1. Chemical Compositions of Coalbed Gas

The coalbed gas composition (Mol%, air free basis) of Longtan Formation in the Dacun Block consists of CH_4, N_2, CO_2, H_2, and heavy hydrocarbon gas (C_{2+}). Among them, CH_4 is the dominated component, with a concentration ranging from 33.8% to 100% (avg. 85.21%). N_2, CO_2, H_2, and C_{2+} account for 0–62.05% (avg. 8.90%), 0–10.92% (avg. 4.97%), 0–1.55% (avg. 0.55%), and 0–8.84% (avg. 0.35%), respectively.

In general, the depth zone where the CH_4 concentration in the coal seam is less than 80% is defined as the CH_4 weathering zone. Figure 3a shows that the CH_4 concentration in the study area, overall, takes on an increasing trend as the depth of coal seam increases. When the depth is more than 310m, the CH_4 concentration of the coal seam is basically more than 80%. Therefore, the CH_4 weathering zone depth of the coal seam in the Dacun Block is 310 m. The N_2 concentration shows a decreasing trend as the depth of the coal seam increases (Figure 3b). Both CO_2 and H_2 concentrations have a poor relationship with the depth of coal seam (Figure 3c,d). With the increase in depth, the C_{2+} concentration in the coal seam presents a parabolic variation of first increasing and then decreasing, and the turning depth is around 550 m (Figure 3e).

Figure 3. The scatter plots between the (**a**) CH_4, (**b**) N_2, (**c**) CO_2, (**d**) H_2, and (**e**) C_{2+} concentrations and the depth of the coal seam in the Dacun Block.
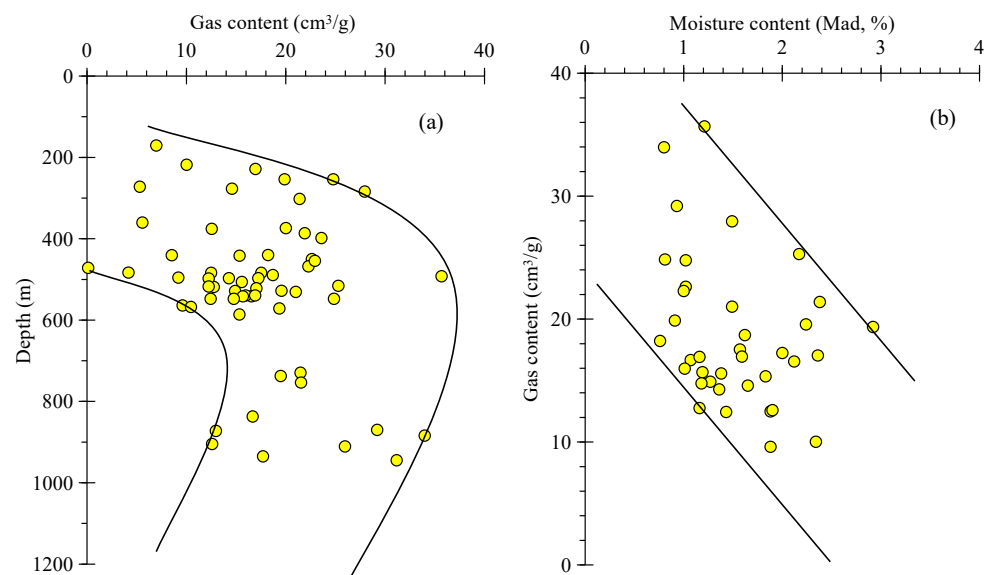
4.2. Gas Content Characteristics

The gas content of the coal seam is the basis of CBM geological evaluation and determines the resource potential of CBM development [40]. The gas contents, referring to CBM contents in this study, of coal seams in the Dacun Block vary from 0.11 to 35.68 cm^3/g, with an average of 17.27 cm^3/g.

Burial depth is one of the important factors affecting the gas content distribution of the coal seam, and its control over the gas content is mainly affected by the temperature and pressure conditions [8]. The influence of temperature and pressure conditions on the adsorbability and even gas content of coal seam presents two different effects [41]. On one hand (positive effect), the adsorption capacity of coals is enhanced with the increase in formation pressure, resulting in the increase in adsorbed gas content; on the other hand (negative effect), the free energy of CBM increases and the adsorption capacity of coal weakens with the increase in formation temperature, leading to the decrease in adsorbed gas content. When the two effects are similar or equal under a specific burial depth, there will be an inflection point in the relationship between adsorbed gas content and burial depth, which is the critical depth. When the depth is greater than the critical depth, the adsorbed gas content of the coal seam gradually decreases. The total gas content usually displays a similar law with the increase in depth as well. In the study area, the total gas
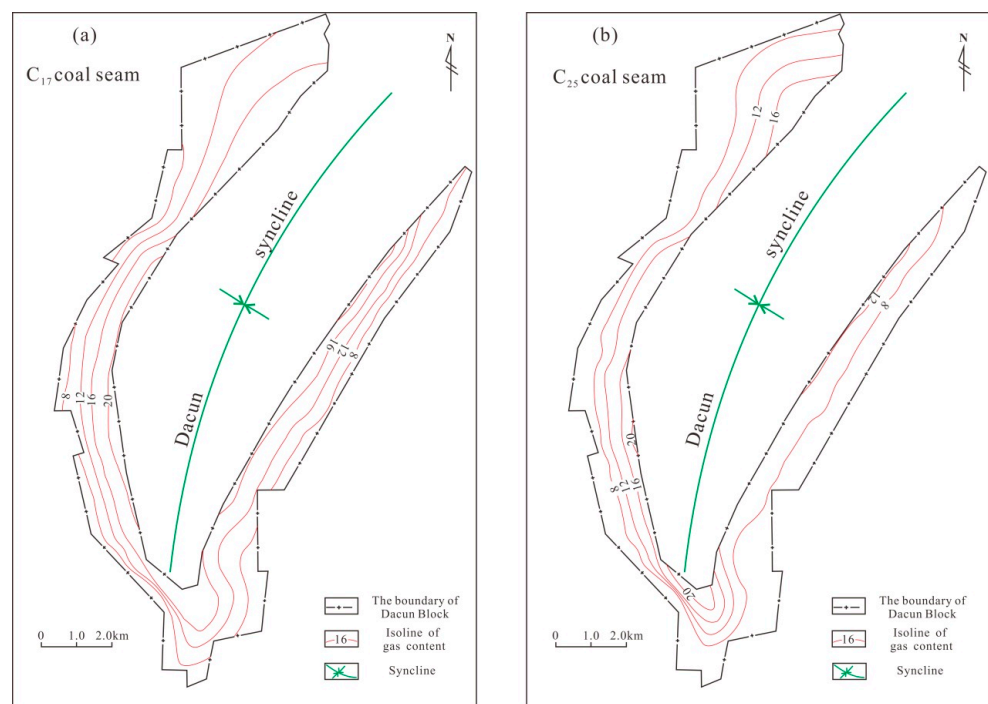
content presents an increasing and then decreasing trend as the depth rises (Figure 4a), and the inflection point (critical depth) is around 700 m.

Figure 4. The relationship between the (**a**) burial depth, (**b**) moisture contents, and gas content of coal seams in the Dacun Block.
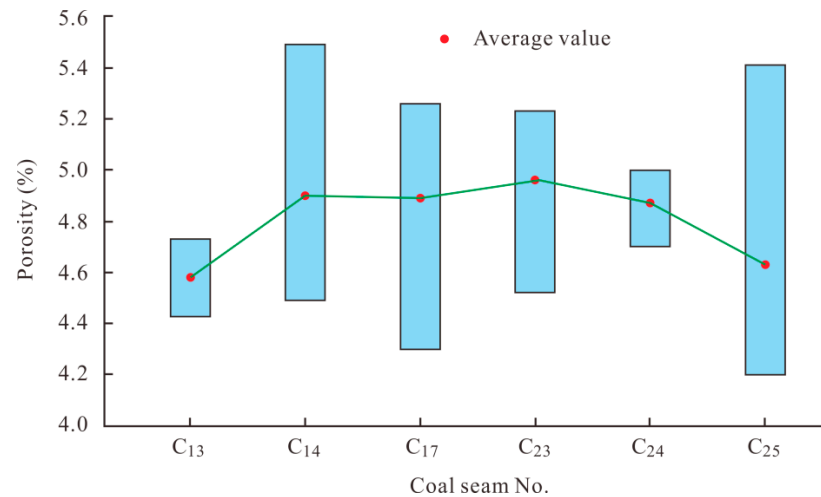
The greater dispersion that exists between burial depth and total gas content is because other factors, such as coal rank, coal composition, coal quality, depositional condition, and structural deformation, may also influence the gas content [22,42]. For example, the moisture contents in coals present a negative relationship with the gas content of coal seams in the study area (Figure 4b). The geological structure also has an obvious influence on the gas content. Taking C_{17} and C_{25} coal seams as examples, the CBM content of coal seams both show an increasing trend from the two limbs to the hinge zone of the Dacun syncline (Figure 5).

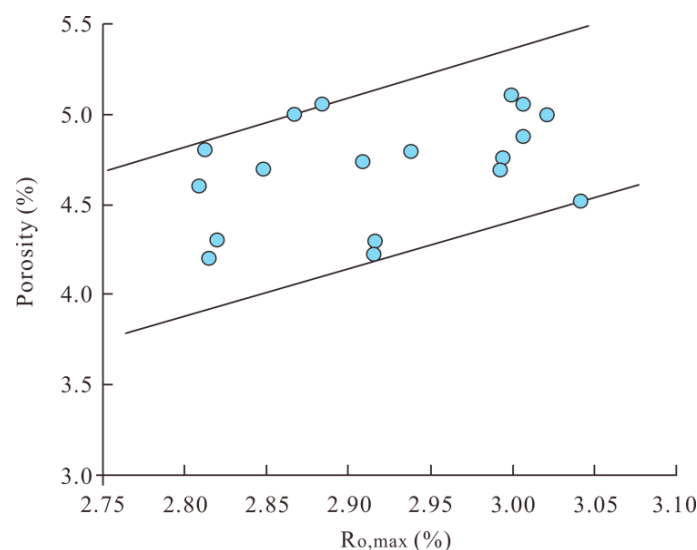**Figure 5.** The gas content isoline of coal seams C_{17} (**a**) and C_{25} (**b**) in the Dacun Block.

4.3. Porosity Characteristics

According to the test results for the helium porosity of coal samples, the porosities of the coal seams in the study area vary from 4.20% to 5.41%, suggesting that the coal seams are low-porosity reservoirs. From the C_{13} to C_{25} coal seam, the average porosities of coal seams increase first and then decrease (Figure 6), reflecting that the coal seams in the middle of P_{3l} may have higher porosities.

Figure 6. Distribution ranges of porosities of different coal seams in the Longtan Formation of the Dacun Block.

Previous studies have shown that the total porosity of coal is closely related to the coal rank. With the increase in coal rank, the total porosity of coal presents a U-shaped curve, and the turning point occurs at $\overline{\overline{R}}r$, approximately 1.6% [43–45]. In other words, starting from lignite, the total pore volume of coal gradually decreases with the increase in the degree of coalification. When it reaches coking coal, the total porosity of coal reaches the minimum value and then gradually increases with the increase in the degree of coalification. The coals in the study area have a high degree of metamorphism, and the maximum vitrinite reflectance ($R_{o,max}$) ranges from 2.59% to 3.10%, with an average of 2.82%, suggesting that the coals are lean-coal to anthracite in rank. Figure 7 shows that the porosity of coal in the study area is positively correlated with the $R_{o,max}$; that is, with the increase in thermal evolution degree, the porosity of coal tends to increase.

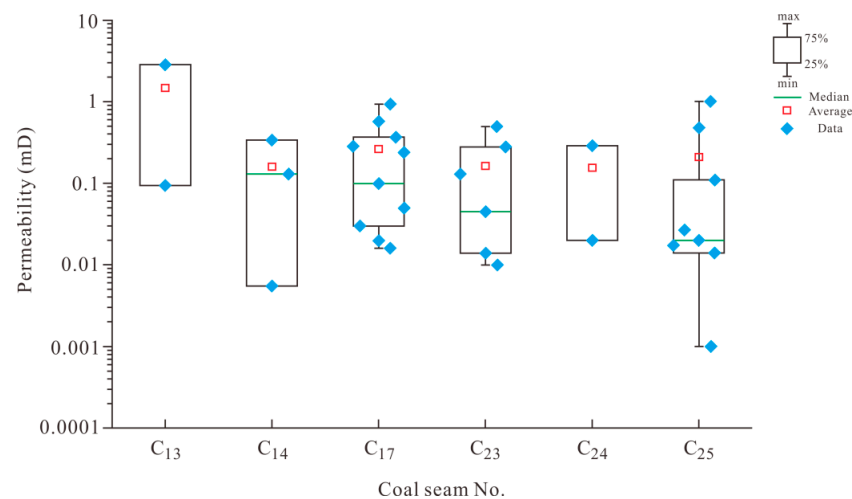**Figure 7.** Relationship between coal porosity and $R_{o,max}$ in the Dacun Block.
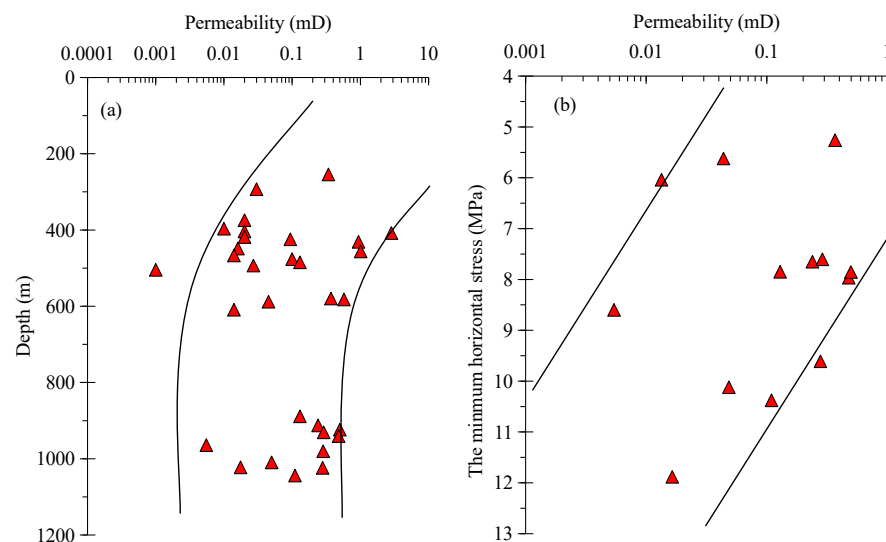
4.4. Permeability Characteristics

Permeability plays an important role in controlling the high yield of CBM [9,29,46]. According to the injection/fall-off well testing results of coal seams, it was found that the permeabilities of coal seams in the study area are very low, ranging from 0.001mD to 2.85 mD (Figure 8), with an average of only 0.29 mD. The permeabilities between different coal seams or even the same coal seam show a strong heterogeneity with greatly variable permeability values (Figure 8). The median permeability from the C_{14} to C_{25} coal seam shows a decreasing trend (Figure 8).

Figure 8. Distribution ranges of well testing permeabilities of different coal seams of the Dacun Block.

The correlation between coal permeability and buried depth in the study area is, overall, low, but it was found that the coal permeability shows a decreasing trend with the increase in buried depth (Figure 9a). Previous studies have shown that present-day stress magnitude and orientation are important reasons for vertical variation in permeability [47–49]. Figure 9b illustrates that a negative relationship exists between coal permeability and minimum horizontal stress magnitude in the study area.
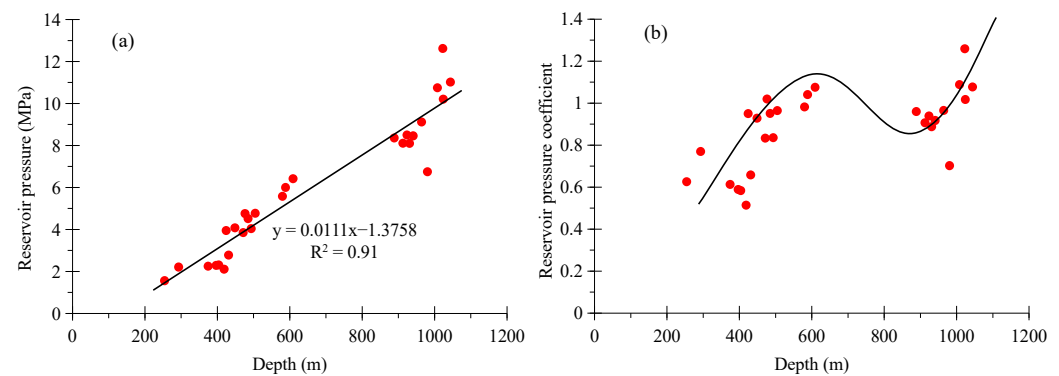

Figure 9. The relationship between the (**a**) burial depth, (**b**) minimum horizontal stress, and permeabilities of coal seams in the Dacun Block.

4.5. Reservoir Pressure Characteristics

Reservoir pressure is the specific form of formation energy, and it not only plays an important role in the content and occurrence state of CBM but also determines the migration and production power of CBM [50]. The injection/fall-off well testing results show that the reservoir pressure of coal seams in the study area varies from 1.56 to 12.62 MPa, with an average of 5.91 MPa. The reservoir pressure coefficient ranges from 0.51 and 1.26, averaging 0.88, and approximately 25% of the coal seams belong to abnormal high-pressure reservoirs. Coal seams with abnormally high pressure are conducive to CBM development. On the one hand, the abnormal high pressure can reduce the stress sensitivity of the coal seam and keep the cleats and fractures open; on the other hand, it can provide stronger migration and output power and larger pressure drop space for CBM during the production process to ensure the production potential and stable production period of the CBM well.

Figure 10a shows that the reservoir pressure of coal seams has a good positive relationship with the depth (R^2 = 0.91). However, the reservoir pressure coefficients of coal seams show a fluctuation change trend (increase→decrease→increase) as the depth increases, and the reservoir pressure coefficient takes on a decreasing trend at the depth between 600 and 900 m (Figure 10b), which reflects that three sets of independent superposed gas-bearing systems possibly exist vertically in the P_{3l} of the study area.
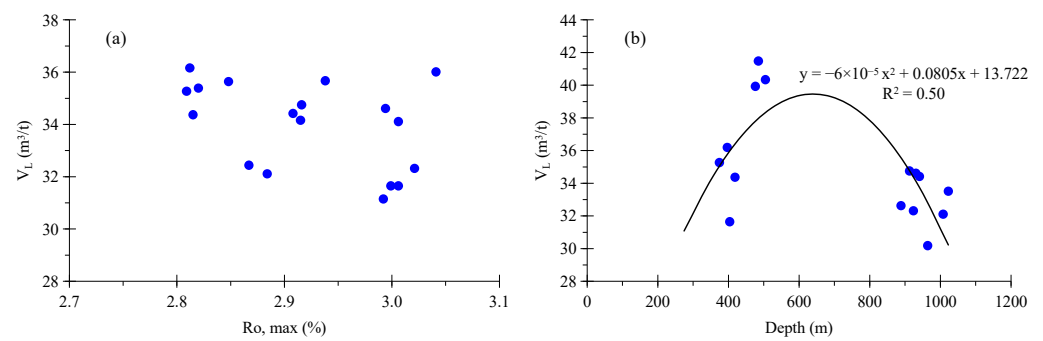

Figure 10. The relationship between the (**a**) reservoir pressure, (**b**) reservoir pressure coefficient, and depth of coal seams in the Dacun Block.

4.6. Adsorption Characteristics

Based on the results of isothermal adsorption experiments under the conditions of equilibrium water and 30 °C, we observe that the Langmuir volumes (V_L) of coal samples in the Dacun Block range from 22.67 to 36.84 m^3/t (avg. 31.36 m^3/t), and the Langmuir pressures (p_L) vary from 0.52 to 1.25 MPa (avg. 1.02 MPa). Fu et al. [51] found that the V_L of coals is rank-dependent. When $R_{o,max}$ < 4.0%, the V_L rises with the increase in $R_{o,max}$, and when $R_{o,max}$ > 4.0%, the V_L decreases with the increase in $R_{o,max}$. However, in this study, the V_L of coal samples seems uncorrelated with the $R_{o,max}$ (Figure 11a), suggesting that the coal rank is not the main controlling factor on the V_L of coals in the Dacun Block.
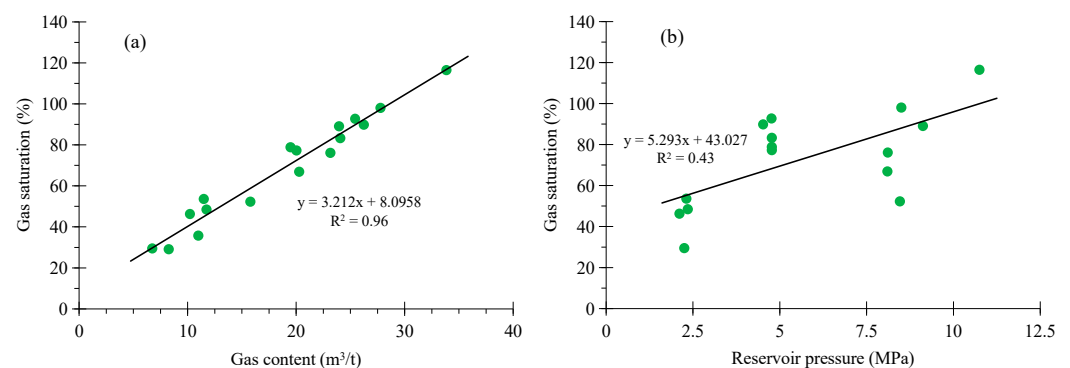
Regardless of coal rank, the V_L of coals in the Dacun Block presents a parabolic change of first increasing and then decreasing with the increase in depth (Figure 11b), and there is a turning depth (critical depth of V_L), which is around 700 m, which is basically consistent with the turning depth of gas content–depth relationship. To be specific, when the depth of the coal seam is shallower than the critical depth, the V_L rises with the increase in depth; once the depth of coal seam exceeds the critical depth, the V_L decreases with the increase in depth. The existence of the critical depth of V_L is an inevitable result of deep geothermal field warming, which is one of the main controlling factors on the adsorptivity of coal under the formation condition [41].

Figure 11. The relationship between the (**a**) $R_{o,max}$, (**b**) depth, and Langmuir volumes (V_L) of coals in the Dacun Block.

4.7. Gas Saturationcharacteristics

Gas saturation is an important parameter for enrichment areas selection and favorable areas prediction of CBM, and it reflects the difficulty of CBM exploitation to a certain extent [15]. Gas saturation is considered to be a more-important geological factor than gas content, affecting the high-yield of CBM wells [52]. The gas saturations of the coal seams in the study area range from 29.10% to 116.48%, with an average of 68.45%. Figure 12a shows that gas saturation is closely related to gas content and rises with the increase in gas content. When the gas contents of coal seams are greater than 20 m^3/t, the gas saturations are higher than 80%. In addition, it was found that the gas saturations of coal seams are positively correlated with the reservoir pressure (Figure 12b), which suggests that the deep coal seams in the study area may have higher gas saturations.

Figure 12. The relationship between the (**a**) gas contents, (**b**) reservoir pressure, and gas saturations of coals in the Dacun Block.
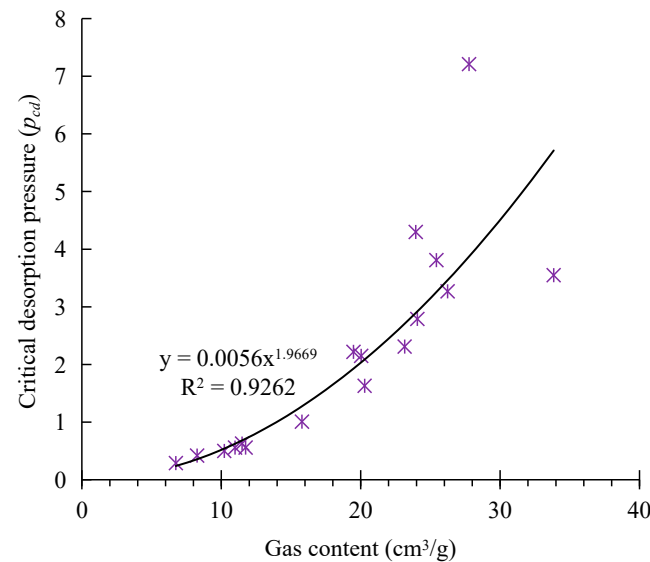
4.8. Critical Desorption Pressure Characteristics

The critical desorption pressure (p_{cd}) of CBM refers to the pressure when desorption and adsorption reach the equilibrium; that is, the pressure when the gas adsorbed on the surface of coal pores and fractures begins the process of desorption [51]. In other words, the p_{cd} is the pressure corresponding to the measured gas content of the coal sample on the isothermal adsorption curve, and its calculation equation is as follows:

$$p_{cd} = \frac{V_a p_L}{V_L - V_a},$$

(2)

where p_{cd} is the critical desorption pressure, in MPa; V_a is the measured gas content of coal seam, in m^3/t; p_L is the Langmuir pressure, in MPa; and V_L is the Langmuir volume, in m^3/t.

The ratio of p_{cd} to reservoir pressure (p) directly determines the difficulty of the drainage and depressurization of CBM. The greater the ratio, the easier it is for CBM to

produce gas. The results show that the p_{cd} of coal reservoirs in the Dacun Block varies from 0.29 to 7.21 MPa, averaging 2.19 MPa. Figure 13 shows that the p_{cd} has a good positive correlation with gas content. The ratio of p_{cd} to reservoir pressure (p) ranges from 0.04 to 0.89, averaging 0.37. It can be seen that the ratio of p_{cd} to reservoir pressure (p) is relatively low, indicating that the CBM development in the Dacun Block needs a large depressurization of reservoir pressure to produce CBM.

$$y = 0.0056x^{1.9669}$$
$$R^2 = 0.9262$$

Figure 13. The relationship between the gas content and the critical desorption pressure (p_{cd}) of the coal reservoir in the Dacun Block.

5. Conclusions

(1) The macrolithotypes of coals in the Dacun block are dominated by semi-dull coals, followed by semi-bright coals. The organic macerals of coals are dominated by vitrinite, followed by inertinite, and exinite is generally rare. The coals are semi-anthracite to anthracite in coal rank.

(2) CH_4 concentration accounts for 33.8–100% (avg. 85.21%) of the total gas component and, overall, takes on an increasing trend as the depth increases. The CH_4 weathering zone depth is 310 m. The coal seams, overall, have a high gas content, varying from 0.11 to 35.68 cm^3/g (avg. 17.27 cm^3/g). The gas content shows a "increase→decrease" trend as the depth increases, and the critical depth is around 700 m.

(3) The coals in the Dacun Block have low porosities (4.20–5.41%) and permeabilities (0.001 mD–2.85 mD). The porosity shows a positive correlation with the $R_{o,max}$. The permeabilities present a decreasing trend with the increase in depth. Moreover, a negative relationship exists between the coal permeability and minimum horizontal stress magnitude.

(4) The coal reservoirs in the Dacun Block overall have a low abnormal pressure state. The fluctuation change relationship between the reservoir pressure coefficient and depth indicates that three sets of independent superposed gas-bearing systems possibly exist vertically in the Longtan Formation.

(5) The coals in the Dacun Block have a strong adsorptivity; however, the gas saturation is low. Coals with high gas contents and reservoir pressures usually have high gas saturations. The CBM development in the Dacun Block needs a large depressurization of reservoir pressure due to the low ratio of critical desorption pressure to reservoir pressure.

References

1. Xie, M.; Yi, X.; Liu, K.; Sun, C.; Kong, Q. How much natural gas does China need: An empirical study from the perspective of energy transition. *Energy* **2023**, *266*, 126357. [CrossRef]
2. Zhang, Y.; Tang, X.Q.; Meng, Q.S.; Wang, W.W.; Huang, W. Development status and prospect of gas distributed energy industry. In *Annual Report on China's Petroleum, Gas and New Energy Industry (2022–2023)*; Springer Nature: Singapore, 2024; pp. 209–227.
3. Xie, M.H.; Wei, X.N.; Chen, C.L.; Sun, C.W. China's natural gas production peak and energy return on investment (EROI): From the perspective of energy security. *Energy Policy* **2022**, *164*, 112913. [CrossRef]
4. Karimpouli, S.; Tahmasebi, P.; Ramandi, H.L. A review of experimental and numerical modeling of digital coalbed methane: Imaging, segmentation, fracture modeling and permeability prediction. *Int. J. Coal Geol.* **2020**, *228*, 103552. [CrossRef]
5. Pashin, J.C. Geology of North American coalbed methane reservoirs. In *Coal Bed Methane*; Elsevier: Amsterdam, The Netherlands, 2020; pp. 35–64.
6. Ray, S.K.; Khan, A.M.; Mohalik, N.K.; Mishra, D.; Mandal, S.; Pandey, J.K. Review of preventive and constructive measures for coal mine explosions: An Indian perspective. *Int. J. Min. Sci. Technol.* **2022**, *32*, 471–485. [CrossRef]
7. Zhao, W.; Wang, K.; Liu, S.; Ju, Y.; Zhou, H.; Fan, L.; Yang, Y.; Cheng, Y.; Zhang, X.A. synchronous difference in dynamic characteristics of adsorption swelling and mechanical compression of coal: Modeling and experiments. *Int. J. Rock Mech. Min. Sci.* **2020**, *135*, 104498. [CrossRef]
8. Li, S.; Qin, Y.; Tang, D.; Shen, J.; Wang, J.; Chen, S. A comprehensive review of deep coalbed methane and recent developments in China. *Int. J. Coal Geol.* **2023**, *279*, 104369. [CrossRef]
9. Qin, Y.; Moore, T.A.; Shen, J.; Yang, Z.; Shen, Y.; Wang, G. Resources and geology of coalbed methane in China: A review. *Int. Geol. Rev.* **2018**, *60*, 777–812. [CrossRef]
10. Xu, F.; Hou, W.; Xiong, X.; Xu, B.; Wu, P.; Wang, H.; Feng, K.; Yun, J.; Li, S.; Zhang, L.; et al. The status and development strategy of coalbed methane industry in China. *Pet. Explor. Dev.* **2023**, *50*, 765–783. [CrossRef]
11. Kang, J.Q.; Fu, X.H.; Elsworth, D.; Liang, S. Vertical heterogeneity of permeability and gas content of ultra-high-thickness coalbed methane reservoirs in the southern margin of the Junggar Basin and its influence on gas production. *J. Nat. Gas Sci. Eng.* **2020**, *81*, 103455. [CrossRef]
12. Chen, S.; Tang, D.; Tao, S.; Liu, P.; Mathews, J.P. Implications of the insitu stress distribution for coalbed methane zonation and hydraulic fracturing in multiple seams, western Guizhou, China. *J. Pet. Sci. Eng.* **2021**, *204*, 108755. [CrossRef]
13. Zhang, Z.; Qin, Y.; Yang, Z.; Li, G.; You, Z. Primary Controlling factors of coalbed methane well productivity and high productive well patterns in Eastern Yunnan and Western Guizhou, China. *Nat. Resour. Res.* **2023**, *32*, 2711–2726. [CrossRef]
14. Yuan, M.; Lyu, S.; Wang, S.; Xu, F.; Yan, X. Macrolithotype controls on natural fracture characteristics of ultra-thick lignite in Erlian Basin, China: Implication for favorable coalbed methane reservoirs. *J. Pet. Sci. Eng.* **2022**, *208*, 109598. [CrossRef]
15. Moore, T.A. Coalbed methane: A review. *Int. J. Coal Geol.* **2012**, *101*, 36–81. [CrossRef]
16. Mostaghimi, P.; Armstrong, R.T.; Gerami, A.; Hu, Y.; Jing, Y.; Kamali, F.; Liu, M.; Liu, Z.; Lu, X.; Ramandi, H.L.; et al. Cleat-scale characterisation of coal: An overview. *J. Nat. Gas Sci. Eng.* **2017**, *39*, 143–160. [CrossRef]
17. Cui, Z.; Zhang, Z.; Huang, W.; Liu, L.; Wang, J.; Wei, X.; Shen, J. Pore-fracture structure characteristics of low-medium rank coals from Eastern Surat Basin by FE-SEM and NMR experiments. *Nat. Resour. Res.* **2024**, *33*, 743–763. [CrossRef]
18. Gan, Q.; Xu, J.; Peng, S.; Yan, F.; Wang, R.; Cai, G. Effect of heating on the molecular carbon structure and the evolution of mechanical properties of briquette coal. *Energy* **2021**, *237*, 121548. [CrossRef]
19. Tang, C.; Yao, Q.; Chen, T.; Shan, C.; Li, J. Effects of water content on mechanical failure behaviors of coal samples. *Geomech. Geophys. Geo-Energy Geo-Resour.* **2022**, *8*, 87. [CrossRef]
20. Karacan, C.; Okandan, E. Assessment of energetic heterogeneity of coals for gas adsorption and its effect on mixture predictions for coalbed methane studies. *Fuel* **2000**, *79*, 1963–1974. [CrossRef]
21. Wang, Z.; Pan, J.; Hou, Q.; Yu, B.; Li, M.; Niu, Q. Anisotropic characteristics of low-rank coal fractures in the Fukang mining area, China. *Fuel* **2018**, *211*, 182–193. [CrossRef]

22. Scott, A.R. Hydrogeologic factors affecting gas content distribution in coalbeds. *Int. J. Coal Geol.* **2002**, *50*, 363–387. [CrossRef]

23. Guo, C.; Xia, Y.; Ma, D.; Sun, X.; Dai, G.; Shen, J.; Chen, Y.; Lu, L. Geological conditions of coalbed methane accumulation in the Hancheng area, southeastern Ordos Basin, China: Implications for coalbed methane high-yield potential. *Energy Explor. Exploit.* **2019**, *37*, 922–944. [CrossRef]

24. Esen, O.; Özer, S.C.; Soylu, A.; Rend, A.R.; Fişne, A. Geological controls on gas content distribution of coal seams in the Kınık coalfield, Soma Basin, Turkey. *Int. J. Coal Geol.* **2020**, *231*, 103602. [CrossRef]

25. Pashin, J.C. Stratigraphy and structure of coalbed methane reservoirs in the United States: An overview. *Int. J. Coal Geol.* **1998**, *35*, 209–240. [CrossRef]

26. Ayers, W.B., Jr. Coalbed gas system, resources, and production and a review of contrasting cases from the San Juan and Powder River basins. *AAPG Bull.* **2002**, *86*, 1853–1890.

27. Chen, Y.; Tang, D.; Xu, H.; Li, Y.; Meng, Y. Structural controls on coalbed methane accumulation and high production models in the eastern margin of Ordos Basin, China. *J. Nat. Gas Sci. Eng.* **2015**, *23*, 524–537. [CrossRef]

28. Zhang, J.Y.; Liu, D.M.; Cai, Y.D.; Pan, Z.J.; Yao, Y.B.; Wang, Y.J. Geological and hydrological controls on the accumulation of coalbed methane within the No.3 coal seam of the southern Qinshui Basin. *Int. J. Coal Geol.* **2017**, *182*, 94–111. [CrossRef]

29. Lv, Y.; Tang, D.; Xu, H.; Luo, H. Production characteristics and the key factors in high-rank coalbed methane fields: A case study on the Fanzhuang Block, Southern Qinshui Basin, China. *Int. J. Coal Geol.* **2012**, *96–97*, 93–108. [CrossRef]

30. Peng, C.; Zou, C.; Zhou, T.; Li, K.; Yang, Y.; Zhang, G.; Wang, W. Factors affecting coalbed methane (CBM) well productivity in the Shizhuangnan block of southern Qinshui basin, North China: Investigation by geophysical log, experiment and production data. *Fuel* **2017**, *191*, 427–441. [CrossRef]

31. Zhang, Z.; Qin, Y.; Zhuang, X.G.; Li, G.Q.; Liu, D.H. Geological controls on the CBM productivity of No.15 coal seam of Carboniferous–Permian Taiyuan Formation in Southern Qinshui Basin and prediction for CBM high-yield potential regions. *Acta Geol. Sin. (Engl. Ed.)* **2018**, *92*, 2310–2332.

32. Yin, Z.S.; Wei, W.J.; Xiao, J.X. CBM exploration and exploitation status, key issues and proposals in Sichuan Province. *Coal Geol. China* **2019**, *31*, 66–69.

33. Liang, W.L.; Wei, W.J.; Deng, Y.P. Upper Permian coal-bearing stratigraphic framework and coal-accumulation in the Guxu coal mine of the south Sichuan Coalfield. *Acta Geol. Sichuan* **2013**, *33*, 287–290.

34. *Chinese Standard SY/T 5336-1996*; Method Core Routine Analysis. Industry standard—Oil: Beijing, China, 1996.

35. *ASTM Standard D3173-11*; Test Method for Moisture in the Analysis Sample of Coal and Coke. ASTM International: West Conshohocken, PA, USA, 2011. [CrossRef]

36. *ASTM Standard D3174-11*; Annual Book of ASTM Standards. Test Method for Ash in the Analysis Sample of Coal and Coke. ASTM International: West Conshohocken, PA, USA, 2011. [CrossRef]

37. *ISO7404.5-1994*; Method for the Petrographic Analysis of Bituminous Coal and Anthracite—Part5: Method of Determining Microscopically the Reflectance of Vitrinite. International Organization for Standardization: Geneva, Switzerland, 1994.

38. *Chinese Standard GB/T 19560-2004*; Experimental Method of High-Pressure Adsorption Isothermal to Coal-Capacity Method. General Administration of Quality Supervision, Inspection and Quarantine of the People's Republic of China: Beijing, China, 2004.

39. Kissell, F.N.; Mcculloch, C.M.; Elder, C.H. The direct method of determining methane content of coals for ventilation design. In *U.S. Bureau of Mines Report of Investigations RI7767*; US Department of Interior, Bureau of Mines: Washington, DC, USA, 1981.

40. Hou, X.; Liu, S.; Zhu, Y.; Yang, Y. Evaluation of gas contents for a multi-seam deep coalbed methane reservoir and their geological controls: Insitu direct method versus indirect method. *Fuel* **2020**, *265*, 116917. [CrossRef]

41. Qin, Y. Progress on geological research of deep coalbed methane in China. *Acta Pet. Sin.* **2023**, *44*, 1791–1811.

42. Guo, Z.; Cao, Y.; Zhang, Z.; Dong, S. Geological controls on the gas content and permeability of coal reservoirs in the Daning Block, Southern Qinshui Basin. *ACS Omega* **2022**, *7*, 17063–17074. [CrossRef]

43. Rodrigues, C.; de Sousa, M.L. The measurement of coal porosity with different gases. *Int. J. Coal Geol.* **2002**, *48*, 245–251. [CrossRef]

44. Mares, T.E.; Radliński, A.P.; Moore, T.A.; Cookson, D.; Thiyagarajan, P.; Ilavsky, J.; Klepp, J. Assessing the potential for CO_2 adsorption in a subbituminous coal, Huntly Coalfield, New Zealand, using small angle scattering techniques. *Int. J. Coal Geol.* **2009**, *77*, 54–68. [CrossRef]

45. Chen, D.; Shi, J.-Q.; Durucan, S.; Korre, A. Gas and water relative permeability in different coals: Model match and new insights. *Int. J. Coal Geol.* **2014**, *122*, 37–49. [CrossRef]

46. Liu, H.H.; Sang, S.X.; Wang, G.G.X.; Li, Y.M.; Li, M.X.; Liu, S.Q. Evaluation of the synergetic gas-enrichment and higher-permeability regions for coalbed methane recovery with a fuzzy model. *Energy* **2012**, *39*, 426–439. [CrossRef]

47. Burra, A.; Esterle, J.S.; Golding, S.D. Horizontal stress anisotropy and effective stress as regulator of coal seam gas zonation in the Sydney Basin, Australia. *Int. J. Coal Geol.* **2014**, *132*, 103–116. [CrossRef]

48. Mukherjee, S.; Rajabi, M.; Esterle, J.; Copley, J. Subsurface fractures, in-situ stress and permeability variations in the Walloon Coal Measures, eastern Surat Basin, Queensland, Australia. *Int. J. Coal Geol.* **2020**, *222*, 103449. [CrossRef]

49. Chen, S.; Tao, S.; Tang, D. Insitu coal permeability and favorable development methods for coalbed methane (CBM) extraction in China: From real data. *Int. J. Coal Geol.* **2024**, *284*, 104472. [CrossRef]

50. Wu, C.; Qin, Y.; Zhou, L. Effective migration system of coalbed methane reservoirs in the southern Qinshui Basin. *Sci. China Earth Sci.* **2014**, *57*, 2978–2984. [CrossRef]

51. Fu, X.H.; Qin, Y.; Wei, C.T. *Coalbed Methane Geology*; China University of Mining and Technology Press: Xuzhou, China, 2007.
52. Qin, Y.; Shen, J.; Shen, Y.L.; Li, G.; Fan, B.H.; Yao, H.P. Geological causes and inspirations for high production of coal measure gas in Surat Basin. *Acta Pet. Sin.* **2019**, *40*, 1147–1157.